Enhancing activity and selectivity in a series of pyrrol-1-yl-1- hydroxypyrazole-based aldose reductase inhibitors: The case of trifluoroacetylation

Nikolaos Papastavrou [a, 1], Maria Chatzopoulou [a, *, 2], Jana Ballekova [b], Mario Cappiello [c], Roberta Moschini [c], Francesco Balestri [c], Alexandros Patsilinakos [d, e], Rino Ragno [d, e], Milan Stefek [b], Ioannis Nicolaou [a, **]

[a] Department of Pharmaceutical Chemistry, School of Pharmacy, Faculty of Health Sciences, Aristotle University of Thessaloniki, 54214 Thessaloniki, Greece
[b] Institute of Experimental Pharmacology and Toxicology, Slovak Academy of Sciences, Dubravska Cesta 9, 841 04 Bratislava, Slovakia
[c] Department of Biology, Biochemistry Unit, University of Pisa, via S. Zeno, 51, Pisa, Italy
[d] Rome Center for Molecular Design, Dipartimento di Chimica e Tecnologie del Farmaco,
Sapienza, Università di Roma, P.le A.Moro 5, 00185 Rome, Italy
[e] Alchemical Dynamics Srl, 00125 Rome, Italy

Aldose reductase (ALR2) has been the target of therapeutic intervention for over 40 years; first, for its role in long-term diabetic complications and more recently as a key mediator in inflammation and cancer. However, efforts to prepare small-molecule aldose reductase inhibitors (ARIs) have mostly yielded carboxylic acids with rather poor pharmacokinetics. To address this limitation, the 1- hydroxypyrazole moiety has been previously established as a bioisostere of acetic acid in a group of aroyl-substituted pyrrolyl derivatives. In the present work, optimization of this new class of ARIs was achieved by the addition of a trifluoroacetyl group on the pyrrole ring. Eight novel compounds were synthesized and tested for their inhibitory activity towards ALR2 and selectivity against aldehyde reductase (ALR1). All compounds proved potent and selective inhibitors of ALR2 (IC50/
ALR2 ¼ 0.043—0.242 mM, Selectivity index ¼ 190—858), whilst retaining a favorable physicochemical
pro le. The most active (4g) and selective (4d) compounds were further evaluated for their ability to inhibit sorbitol formation in rat lenses ex vivo and to exhibit substrate-specific inhibition

Introduction

Since its initial discovery in 1956 [1], aldose reductase (ALR2; EC 1.1.1.21) has been established as a prominent factor for the onset and progression of diabetes mellitus' long-term complications, such as neuropathy, nephropathy, cataracts and vascular pathol- ogies to name a few [2]. ALR2 catalyzes the NADPH-dependent reduction of glucose to sorbitol in the first and rate-limiting step of the "polyol pathway", before sorbitol dehydrogenase (SDH) ox- idizes it to fructose [3]. Under normoglycemia, the polyol pathway accounts for just 3% of glucose metabolism. However, in diabetic patients this figure may rise up to 33% and lead to various cellular stress conditions (e.g. osmotic, oxidative, PKC stress), which pro- vide the underlying mechanism for long-term diabetic complica- tions [4,5]. More recently, ALR2 has been identified as a key mediator in a number of inflammation-induced pathologies, ranging from sepsisand asthma to various types of cancer (e.g. colon, breast, ovarian, prostate, lung) [6,7]. The physiological role of aldose reductase in the reduction of toxic aldehydes [8] is also the key step in the manifestation and propagation of oxidative-stress induced inflammation. 4-hydroxy-2- nonenal (HNE), a product of lipid per- oxidation, and its glutathione adduct (GS-HNE) are converted by ALR2 to 1,4-dihydroxynonene (DHN) and glutathionyl-1,2- dihydroxynonene (GS-DHN), respectively. A cascade of kinases (PLC, PKC, MAPK) and transcription factors (NF-kB, AP-1) are in turn
activated, leading to the production of pro-inflammatory signals (iNOS, chemokines, cytokines, growth factors) [9].Considering the large spectrum of ALR2- related pathologies, aldose reductase inhibitors (ARIs) hold great promise for thera- peutic intervention. Over the last 40 years a wide variety of syn-

thetic and natural product-derived inhibitors has been discovered, and the field attracts a lot of interest to this day [10e12]. Efforts to market these inhibitors, however, have been met with limited success. To date, only one compound, epalrestat, is commercially available in Japan and India for the treatment of diabetic neurop-athy, following the withdrawal of tolrestat from Europe in 1990. Epalrestat showed marginal clinical efficacy and thus has not received FDA or EMEA approval. Both these inhibitors are carbox- ylic acid derivatives and together with spiroimides (sorbinil, ranirestat) comprise the two main classes of ARIs (Fig. 1A). Car- boxylic acids are potent inhibitors thanks to the high affinity for the positively charged region of the ALR2 active site. At the same time, low pK_a values hinder membrane permeability in physiological pH conditions and lead to a poor pharmacokinetic profile. On the other hand, adverse side effects, such as hypersensitivity (typical of the hydantoin class) and hepatotoxicity, are the major obstacles faced by spiroimides during clinical trials. Off-target inhibition of the closely related aldehyde reductase enzyme (ALR1; EC 1.1.1.2) is thought to be the cause of these side effects [13,14]. Moreover, the above mentioned involvement of ALR2 in detoxification reactions and in the inflammatory cascade led to the proposal of a "differ- ential inhibition" approach to target the enzyme. That is to inhibit damaging ALR2 catalyzed reactions (i.e. reduction of glucose and GS-HNE) without interfering with the beneficial action of the enzyme (i.e. reduction of toxic alkanals and alkenals) [15].

Previously, we identified the 1-hydroxypyrazole moiety as an acetic acid bioisostere in a series of pyrrol-1-yl-acetic acids [16]. This moiety endowed the inhibitors with sub-micromolar activity and a higher pK_a value compared to the acetic acid derivatives. In addition, the high selectivity exhibited by this scaffold (compared to the tetrazole or 2,6-difluorophenol bioisosteres previously re- ported [17,18]) probed us to further optimize this group of ARIs. Based on the observation that the introduction of the di- and tri- fluoroacetyl moiety on the 2-position of the pyrrole ring increased the inhibitory activity towards ALR2, because of important in- teractions with the co-factor, as well as key amino acids (Trp20, Tyr48 and His110) in the enzyme's active site, we set out to study its effect on our pyrrol-1-yl-1-hydroxypyrazole scaffold [19,20]. To that end, we designed and synthesized several compounds bearing a trifluoroacetyl group on the 2'-position of the pyrrole ring and different para- or meta-substituted aroyl moieties on the 4'-posi- tion (Fig. 1B). Their inhibitory activity towards ALR2 and selectivity against ALR1 was tested in vitro, whilst the most potent compounds were also tested in an ex vivo protocol to assess their ability to inhibit sorbitol formation in rat lenses. Finally, a kinetic charac- terization of the most active compound was also carried out on the human recombinant enzyme.
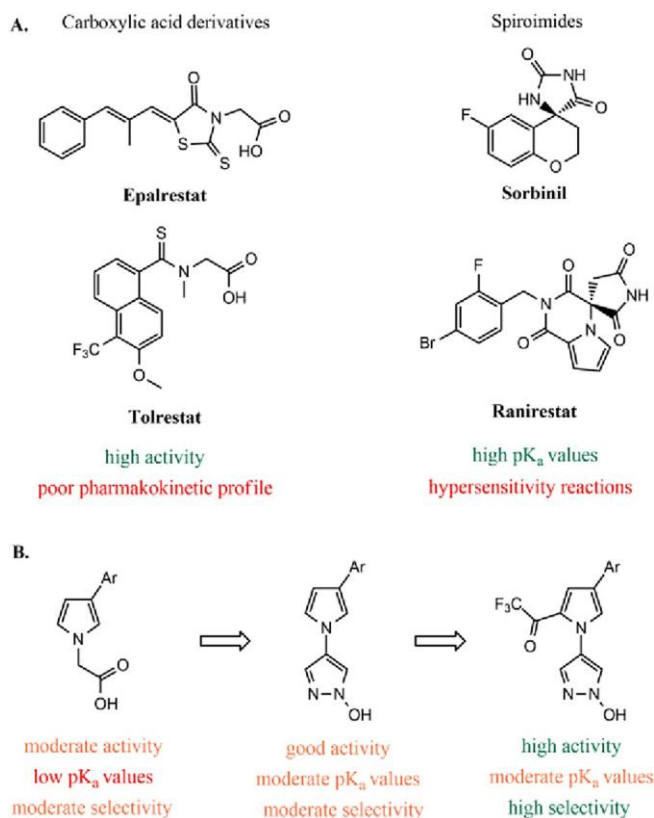
Fig. 1. A. Representative examples of the two main classes of ARIs with the advantages and drawbacks of each class underneath. B. Optimization route of pyrrolyl-based ARIs and key attributes of each step.

1. Results and discussion

1.1. Chemistry

The synthetic route employed for the synthesis of compounds 4a-h is outlined in Scheme 1. Experimental data on compounds 1a- c [21] and 2a-c [16] is reported elsewhere.

The first step included the Friedel-Crafts aroylation of 1- benzenesulfonyl-1H-pyrrole with the appropriate aroyl chloride and subsequent alkaline hydrolysis. Compounds 1d-f were isolated

in very good yields (84e85%), as opposed to 1g (45%). The latter is

in agreement with our previous observation [22] that acylation with electron rich aroyl chlorides gives rise to a mixture of 2'- and 3'-isomers. Next, pyrroles 1d-g were coupled with 1-(benzyloxy)- 4-iodo-1H-pyrazole [16] in a modified Ullman type reaction [21] using CuI as a catalyst to afford the respective pyrrol-1-yl-1-

pyrazoles 2d-g in high yields (79e94%).

Trifluoroacetylation of compounds 2a-g with trifluoroacetic anhydride in 1,2-dichloroethane led to the synthesis of bis- substituted pyrroles 3a-h. This reaction was first carried out using conventional heating (reflux) and 2a as a model compound, which yielded 60% of the corresponding trifluoroacetylated derivative 3a after 24 h. Thus, microwave irradiation was selected as an alter- native method and then optimized to increase the yield to 93%.

Microwave heating also led to fewer side-products and faster re- action times (1e2 h). Deprotection of benzyl ethers 3a-h in concentrated H_2SO_4 afforded target compounds 4a-h in good yields. An acidic deprotection [23] was favored over the previously used hydrogenolysis reaction [16] due to the faster reaction time

(30 min) and easier work-up.

Finally, oxidation of sulfide 2g to sulfone 2h was achieved by treatment with m-CPBA in a moderate yield (46%) [24].
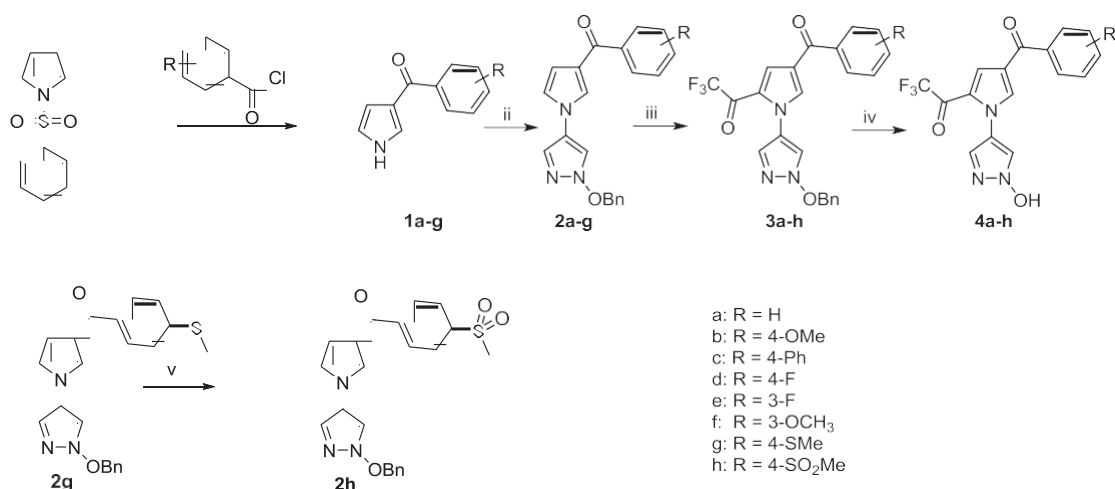
Scheme 1. 1A. Synthetic route for the synthesis of trifluoromethylated pyrrol-1-yl-1-hydroxypyrazoles 4a-h: i. AlCl$_3$, ClCH$_2$CH$_2$Cl, rt, 1.5 h; NaOH 5 N, dioxane, rt, 16 h; ii. 1-(benzyloxy)-4-iodo-1*H*-pyrazole, *trans-N,N'*-dimethylcyclohexane-1,2-diamine, CuI, K$_3$PO$_4$, toluene, reflux, 24 h; iii. (CF$_3$CO)$_2$O, ClCH$_2$CH$_2$Cl, MW (Power ¼ 300 W, Temp. ¼ 120 °C); iv. conc. H$_2$SO$_4$, 60 °C, 30 min; 1B. Synthesis of oxidized intermediate 2h. v. *m*-CPBA, DCM, rt, 18 h.

1.2. *ALR2/ALR1 inhibitory activity and docking simulation*

Introduction of the trifluoroacetyl group in the pyrrole ring increased ALR2 inhibitory activity by five-to tenfold. This is consistent with our previous study of 2-fluorophenol derivatives [19], where a 10fold increase was also observed. In general, all the synthesized analogs inhibited ALR2 in submicromolar concentra- tions (Table 1), proving more potent than the control compound sorbinil (IC$_{50}$ 0.25 mM [25]). Furthermore, substitution on the phenyl ring had a positive influence on activity. More specifically, the p-methoxy, p-phenyl and p-fluoro derivatives (4b, 4c and 4d)

were active in the range of 73e78 nM. Isosteric replacement of the oxygen atom in the methoxy group with sulfur led to the most active derivative, sulfide 4g, with an IC$_{50}$ of 43 nM. Studies support the beneficial influence of non-oxidized sulfur atoms in drug development, as they can participate in interactions with electron donating atoms both inter- and intramolecularly [26]. Interestingly, its potential oxidized metabolite, the sulfone derivative 4h, also inhibited ALR2, but to a lesser extent in comparison to the sulfide. The same profile is also present in other ARIs, such as sulindac sulfide and sulfone [27]. Finally, substitutions in the meta position led to a similarly active compound in the case of the methoxy derivative 4f, whereas a slight loss of activity was observed in the case of m-fluoro derivative 4e.

The selectivity of the synthesized compounds was assessed against the homologous enzyme aldehyde reductase (ALR1). The two enzymes have a 65% sequence similarity and are structurally homologous [28]. This sub-series proved to be the most selective among the phenyl(1*H*-pyrrolyl)methanones [16e19,29]. All the analogs were more selective for ALR2 against ALR1, with a selec- tivity index (SI) over 190 and up to 858. The most selective analog in this series was the p-fluoro 4d, followed closely by the sulfone (4h, SI: 775) and the sulfide (4g, SI: 650). Surprisingly, the least selective analog in this series was the biphenyl 4c, in contrast to our previous work [16], where the biphenyl was the most active and selective in both the hydroxypyrazole and the acetic acid series.

To investigate the binding mode in this series of compounds, a docking simulation study was run. Autodock Vina (Vina) [30,31] was found suitable as program to perform molecular docking simulations of ligands into ALR2 in a previous study [19]. Therefore, Vina was used to investigate the binding mode of titled derivatives 4a-h by means of a cross-docking procedure [32] using seven ALR2 experimental structures retrieved from PDB (www.rcsb.org).

The 4a-h putative binding modes were inspected, and all showed binding modes overlapping with those of the co- crystallized ligands (not shown). To avoid redundancy, herein de- tails are reported only for the most active derivative 4g. The binding mode observed, overlaps with that of a previously described analog bearing a 3-fluoro-4-hydroxyphenyl (compound 31 in Ref. [19]) in place of 4g's 1-hydroxypyrazolyl moiety (Fig. 2).

In particular, the benzoyl moiety fills up the aromatic rich pocket formed by Trp79, Cys80, Trp111, Thr113, Phe115, Cys303, Tyr309, Pro310 and Phe311 side chains (Fig. 2). The trifluoroacetyl group is involved in positive steric interactions with the NADP nicotinamide group and three surrounding residues' side chains (Trp20, Tyr48 and His120), while the carbonyl makes a weak hydrogen bonding with Cys298 side chain. Finally, the N1 pyrrole 1- hydroxypyrazole ring is placed in the active site entrance channel, making van der Waals interactions with Trp20, Val47, Phe122 and Trp219 side chains. No relevant interactions were observable for the benzoyl carbonyl moiety.
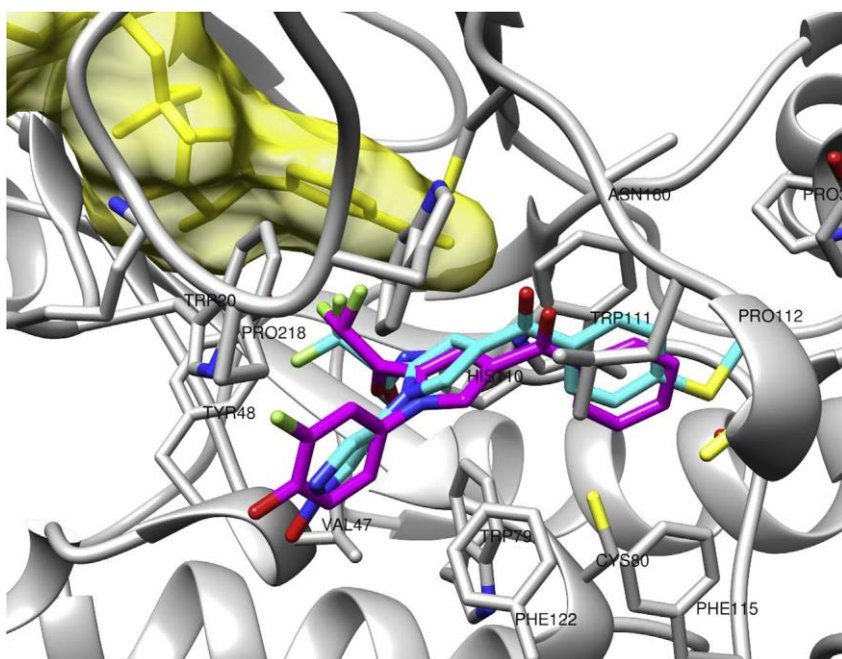
Fig. 2. 4g (cyan) docked conformation in ALR2 (PDB entry code 3T42). For comparison, docked conformation of compound 31 in Ref. [19] (magenta) is also depicted. NAPD is depicted in yellow. (For interpretation of the references to colour in this figure legend, the reader is referred to the web version of this article.)

13. Inhibition of sorbitol formation in rat lenses

As shown in Fig. 3, a marked accumulation of sorbitol was demonstrated in the rat eye lenses cultivated in the presence of high glucose under *ex vivo* conditions. This increase in the lens sorbitol levels was significantly attenuated in the presence of compounds 4d and 4g, at concentrations as low as 10 mM. At 50 mM, the inhibition amounted to approximately 55% for both compounds studied. Evidently, the overall effect recorded in the intact organ

reflects the combination of bioavailability determinants (lip- ophilicity plus polar surface area) with inhibitory activity.
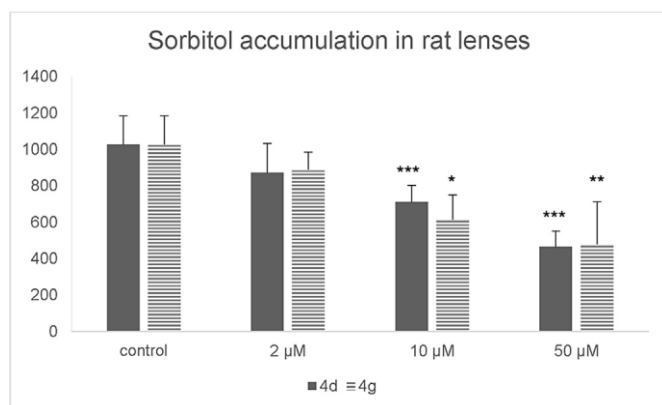

Fig. 3. Sorbitol accumulation in isolated rat lenses incubated in the presence of high glucose (50 mM) and different concentrations of 4d and 4g. Results are mean values ± SD from n ¼ 3e9 independent incubations. *p < 0.1 vs control, **p < 0.01 vs. control, ***p < 0.001 vs. control; one way ANOVA.

14. Enzyme kinetics

In order to further examine the inhibitory profile of the most active ARIs, kinetic analysis was performed for 4d and 4g by using a highly purified preparation of hALR2. GAL (D,L-glyceraldehyde) and, due to their relevance as substrates for the enzyme, HNE, GS- HNE and ʟ-idose, an alternative substrate for ᴅ-glucose [33], were used for the analysis. The inhibitory action of 4g on the reduction of the above substrates is represented through Hanes-Woolf plots in Fig. 4. Secondary plots of $1/^{app}V_{max}$ and $^{app}K_M/^{app}V_{max}$ vs inhibitor concentration have been used to evaluate the dissociation con- stants K_i and K_i', related to the interaction with the free enzyme and with the enzyme-substrate complex, respectively. Similar results coming from the analysis for 4d are reported in the ESI Section (ESI Fig. 1 to ESI Fig. 4). The emerging inhibition constants for the in- hibitors acting on the reduction of the above four different sub- strates are reported in Table 2.

Both compounds displayed a mixed type of inhibition with a prevailing uncompetitive action with respect to ʟ-idose (K_i/K_i' of

12.30 and 16.25 for 4d and 4g, respectively), HNE (K_i/K_i' of 2.67 and 9.82 for 4d and 4g, respectively) and GAL (K_i/K_i' of 6.43 and 9.57 for 4d and 4g, respectively). A more balanced action of both inhibitors in targeting the free enzyme or the enzyme substrate complex was observed for the GS-HNE reduction. In this case the K_i/K_i' ratios accounted approximately for 0.75 for both 4d and 4g.

Looking at the absolute values of the dissociation constants (Table 2), 4g appears to target the human recombinant enzyme as the most effective inhibitor. It may be worth noting, however, that 4d, even though less effective in absolute terms, appears to pref- erentially act on L-idose (K_i' 0.70) with respect to HNE (K_i' 2.19). Unfortunately, the fact that this difference concerns the interaction of the inhibitor with the ALR2-substrate complex, makes it less useful in determining an effective differential inhibitory action of the molecule [34].

A final comparison among the effect of 4g on GS-HNE and HNE is also worth noting. Both the absolute and relative values of K_i and K_i' for GS-HNE make the reduction of this particular substrate effi- ciently inhibited, irrespectively of substrate concentration. On the contrary, HNE reduction is driven through a preferential action on the enzyme-substrate complex. Thus, the inhibition of the detoxi- fying action of ALR2 should occur only at high, improbable, concentration of HNE.

A differential inhibition between GS-HNE and HNE should be beneficial by reducing the ALR2 dependent inflammation signaling without interfering with the ALR2-linked HNE detoxification [15]. Even though 4g exhibits only partial differential inhibition between the two substrates, it could serve as a starting point for future ef- forts aiming at enhancing this feature and delivering ALR2 in- hibitors with improved anti-inflammatory properties.
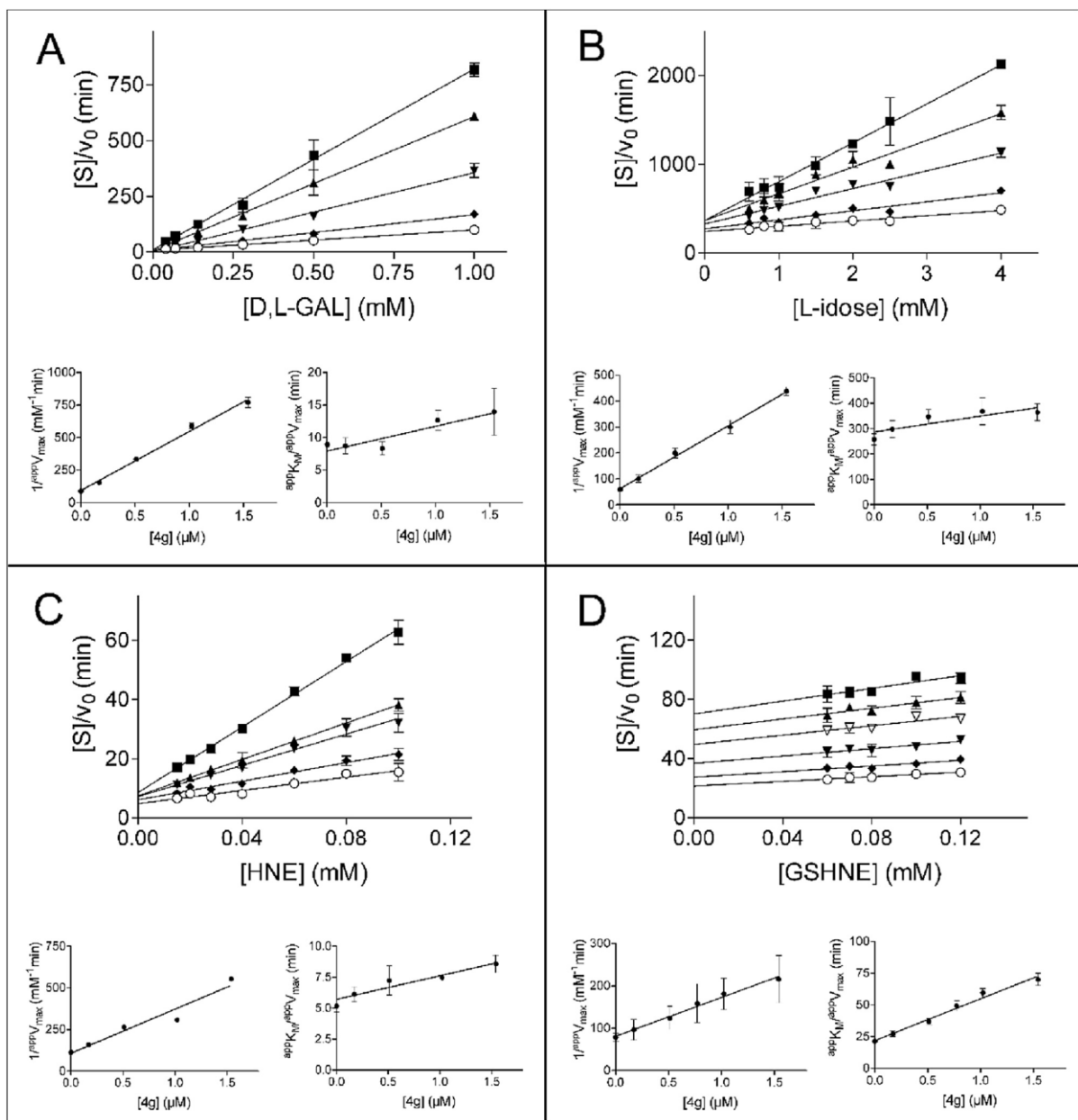

Fig. 4. Kinetic characterization of 4g as h-ALR2 inhibitor. The activity of purified hALR2 (8 mU) was measured at the indicated concentrations of different substrates in the absence (B) or in the presence of the following concentrations of the inhibitor: (A) 0.17 mM, ( ) 0.51 mM, (▽ 0.77 mM, ( ) 1.02 mM, (—) 1.54 mM. Panels A, B, C and D refer to the reduction of GAL, L-idose, HNE and GS-HNE, respectively. In each panel, the upper graph refers to the Hanes-Woolf plot representation of the reduction of the indicated substrate. The lower graphs of each panel refer to the secondary plots of the slopes ($1/^{app}V_{max}$) and the ordinate intercept ($^{app}V_{max}/^{app}K_M$) of the relative Hanes-Woolf plot, as a function of the inhibitor concentration, in order to evaluate K_i' and K_i, respectively. Error bars (when not visible are within the symbols size) represent the standard deviations of the mean from at least three independent measurements.

1.5. Physicochemical profile

An increase in lipophilicity is quite common during the opti- mization step in lead discovery. This stems from trying to solely improve the lead's potency, without taking into account the rest of the properties that are important for biodistribution and for the compound's fate in the organism. In this series, it is of importance, that apart from activity and selectivity, the introduction of the trifluoroacetyl group significantly improved the physicochemical properties (Table 3). All new analogs adhere to Lipinski's rule of 5, but more importantly, they have molecular obesity indices in the favored range for lead compounds and drug candidates. Ligand efficiency (LE) and binding efficiency index (BEI) are both higher than the proposed values for successful leads. Both indices correct IC_{50} for molecular size and should be conserved or increase during the process of a successful optimization. It is noteworthy that LE values are conserved when compared to our previous work [16], however lipophilic ligand efficiency (LLE) has increased signifi- cantly in this sub-series. LLE is a molecular obesity index that separates the contributions of non-specific from specific binding to a molecular target. As such, increased LLE values are indicative of enthalpy-driven optimization and this is associated with an improved ADMET profile, based both on lowered lipophilicity and increased specificity [35]. This is further supported by the fact that lipophilicity-corrected ligand efficiency (LELP) values are also in the optimal range for successful leads, with the exception of the biphenyl analog 4f. Finally, oral bioavailability is predicted to be favorable, as total polar surface area (TPSA) values in the range of 60e120 $Å^2$ suggest good passive absorption [36].

Table 2
Inhibition dissociation constants (mM) for 4d and 4g.

Cpd		Substrate			
		GAL	L-idose	HNE	GSHNE
4d					
	Ki'	0.82 ±0.02	0.70 ± 0.11	2.19 ± 0.04	2.46 ± 0.25
	Ki	5.27 ± 0.53	8.61 ± 0.91	5.84 ± 0.41	1.86 ± 0.13
4g					
	Ki'	0.21 ± 0.01	0.27 ± 0.06	0.39 ± 0.05	0.93 ±0.02
	Ki	2.01 ±0.42	4.55 ±1.10	2.83 ± 0.95	0.69 ± 0.01

Table 3
Physicochemical properties and molecular obesity indices.

Cpd	MW (KDa)	pIC50	logP[a]	logD7.4[a]	LE[b]	BEI[c]	LLE[d]	LELP[e]	TPSA (Å²)[f]
Optimal values	<500		1e5	0e3	0.39[g]	>12.4	3.78[g]	8.82[g]	60e120
4a	349.27	6.62	2.442	0.738	0.37	18.94	4.17	6.59	77.13
4b	379.30	7.14	2.643	0.644	0.37	18.82	4.49	7.14	86.36
4c	379.30	7.19	2.500	0.455	0.37	18.97	4.69	6.70	86.36
4d	367.26	7.11	2.652	0.732	0.38	19.35	4.46	6.93	77.13
4e	367.26	6.85	2.531	0.587	0.37	18.66	4.32	6.86	77.13
4f	425.37	7.13	4.162	1.928	0.32	16.76	2.97	12.92	77.13
4g	395.36	7.37	3.022	1.065	0.38	18.63	4.34	7.91	77.13
4h	427.36	7.03	1.972	0.511	0.34	16.44	5.05	5.81	111.27

[a] S þ logD7.4 and S þ logP values were computationally calculated with MedChem Designer™ Version 1.0.1.15, Copyright © 2011 Simulations Plus, Inc. [www.simulations- plus.com] and correspond to the S logD and S logP values respectively, logD represents the logarithm of the octanol -buffer[pH 7.4] distribution coefficient.
[b] Ligand efficiency calculated as LE ¼ 1.4log(IC_{50})/N, N: number of heavy atoms.
[c] Binding efficiency index calculated as BEI ¼ pIC50/MW.
[d] Lipophilic ligand efficiency calculated as LLE ¼ pIC50 e logP.
[e] Llipophilicity-corrected ligand efficiency calculated as LELP ¼ logP/LE.
[f] Total polar surface area (TPSA) values calculated using the online software http://www.daylight.com/meetings/emug00/Ertl/.
[g] Mean values for successful leads [35,37].

2. Conclusion

In summary, the microwave-assisted introduction of a tri- fluoroacetyl group in a series of aryl-substituted pyrrol-1-yl-1-hydroxypyrazoles was achieved. Eight novel compounds were synthesized with increased ALR2 inhibitory activity and higher selectivity compared to their mono-substituted counterparts, re- ported previously. Furthermore, the physicochemical profile of this series, generated in silico, was improved and appeared in an optimal range for drug candidates. The most active and selective compounds, 4g and 4d respectively, were also potent inhibitors of sorbitol accumulation in rat lenses ex vivo, further suggesting the concurrent ability of the compounds for effective membrane permeation and ALR2 inhibition. Finally, the mode of inhibition of compounds 4d and 4g was evaluated against several different substrates, revealing, for the human enzyme, a preferential inhi - bition of GS-HNE reduction in respect to the HNE.

3. Experimental

3.1. Chemistry

General: All reagents were purchased from SigmaeAldrich Co. and used without further purification, except for the solvents used for flash chromatography and recrystallization. NMR spectra were recorded on an Agilent 500/54 (DD2) spectrometer (500 MHz for ^{1}H NMR, 125 MHz for ^{13}C NMR), and chemical shifts are given in d, referenced to the residual solvent peak. UVeVis measurements were taken with a UV/Vis spectrometer Lambda 20. Melting points are uncorrected and were determined in open glass capillaries using a Mel-Temp II apparatus. Elemental analyses were performed by a PerkineElmer 2400 CHN analyzer (in the Department of Organic Chemistry, School of Chemistry, Aristotle University of Thessaloniki). Flash column chromatography was carried out with Merck silica gel 60 (230e400 Mesh ASTM). TLC was run with Fluka Silica gel/TLC-cards. All solvents used for column chromatography and/or recrystallization were routinely distilled prior to use. Pe- troleum ether refers to the fraction with bp 40 e 60 $^{\circ}$C.

3.1.1. General procedure A: Friedel-Crafts aroylation and alkaline hydrolysis (1d-g)

To a suspension of $AlCl_3$ (1.16 g, 8.68 mmol) in 1,2- dichloroethane (15 mL) under an inert atmosphere, the appro- priate aroyl chloride (8.1 mmol) was added slowly and the resulting mixture was stirred at room temperature for 15 min. A solution of 1-benzenesulfonyl-1*H*-pyrrole (1.5 g, 7.24 mmol) in 1,2- dichloroethane (3 mL) was added and the mixture was allowed to stir at room temperature for 90 min. The reaction mixture was quenched with equal parts of ice and water over 30 min. The aqueous phase was extracted with DCM (2 30 mL) and the combined organic extracts were washed with brine, dried over anh. Na_2SO_4 and concentrated under reduced pressure. The resulting residue was dissolved in dioxane (30 mL) and to this a 5 N NaOH solution (30 mL) was added. The reaction mixture was vigorously stirred overnight at room temperature. The aqueous layer was then extracted with EtOAc (3 × 30 mL) and the combined organic layers were washed with brine, dried over anh. Na_2SO_4 and concentrated under reduced pressure. The residue was purified by silica gel column chromatography (10e25% EtOAc in petroleum ether).

3.1.2. General procedure B: modified Ullman type coupling (2d-g)

To a stirred solution of compound A (800 mg, 2.66 mmol) in dry toluene, (4 mL) the appropriate 3-aroyl-(1*H*)-pyrrole (2.21 mmol), *trans-N,N'*-dimethylcyclohexane-1,2-diamine (64 mg, 0.49 mmol), K_3PO_4 (985 mg, 4.64 mmol) and CuI (21 mg, 0.11 mmol) were added in that order. The resulting mixture was refluxed for 24 h under a nitrogen atmosphere. The reaction mixture was diluted with DCM and filtered through a plug of silica. The silica was washed with ample DCM and EtOAc and the solvents were removed under reduced pressure. The residue was purified by silica gel column chromatography (15e20% EtOAc in petroleum ether).

3.1.3. General procedure C: microwave-assisted pyrrole trifluoroacetylation (3a-h)

To a solution of the appropriate pyrrol-1-yl-1-pyrazole (0.83 mmol) in 1,2-dichloroethane (2.3 mL) was added $(CF_3CO)_2O$ (1.88 g, 8.94 mmol). The mixture was transferred to a 10 mL vial, sealed with a crimp cap and placed in a CEM Discover Lab Mate reactor microwave cavity. The resulting mixture was irradiated at 120 $^{\circ}$C for 8 15 min (Power: 300 Watt), with cooling by com- pressed air in the intermediate stages between two cycles. The reaction mixture was quenched with ice/water, followed by extraction with DCM (2 × 15 mL). The combined organic layers were washed with brine, dried over anh. Na_2SO_4 and concentrated under reduced pressure. The residue was purified by silica gel column chromatography (5e15% EtOAc in petroleum ether).

3.1.4. General procedure D: Benzyl deprotection in conc. H_2SO_4 (4a-h)

The corresponding benzyl ether (0.20 mmol) was dissolved in conc. H2SO4 (5 mL) and the reaction mixture was placed in an oil bath at 60 oC for 30 min. The resulting solution was poured over ice/ water (25 mL) and stirred vigorously for 15 min, followed by extraction with Et2O (3 30 mL). The organic layers were collected and concentrated under reduced pressure. The residue was recrystallized from DCM/petroleum ether.

3.1.5. (1-(1-(benzyloxy)-1H-pyrazol-4-yl)-1H-pyrrol-3-yl) (4- (methylsulfonyl)phenyl)methanone (2h)

To a stirred solution of compound 2g (500 mg, 1.28 mmol) in DCM (5 mL), m-CPBA (77% max purity, 866 mg, 3.86 mmol) was added in portions at ambient temperature. The resulting mixture was allowed to stir overnight, followed by sequential washing with 5% $NaHCO_3$, water and brine. The organic layer was dried over anh. Na_2SO_4 and concentrated under reduced pressure. Silica gel column chromatography afforded 248 mg of the title compound (yield:46%). mp: 144e145 $^{\circ}$C; ^{1}H NMR (C*D*Cl_3): 8.07e8.02 (m, 2H), 7.99e7.94 (m, 2H), 7.41e7.36 (m, 4H), 7.35e7.30 (m, 2H), 7.29e7.26(m, 1H), 7.17e7.15 (m, 1H), 6.81e6.77 (m, 1H), 6.75e6.72 (m, 1H), 5.33 (s, 2H), 3.10 (s, 3H); ^{13}C NMR (C*D*Cl_3): 188.7, 144.4, 142.8, 133.2, 129.7, 129.6, 129.4, 128.8, 127.4, 127.1, 125.9, 125.0, 122.7, 121.6, 116.2, 111.8, 80.8, 44.4. Analysis calculated for $C_{22}H_{19}N_3O_4S$: C, 62.69; H, 4.54; N, 9.97, found: C, 62.45; H, 4.61; N, 9.89.

4.2. Rat ALR2/ALR1 inhibitory activity

Enzyme preparation along with inhibitory activity determina- tion were performed as described before [19] (ESI).

4.3. Computational methods, docking simulations

All calculations were performed with the same protocol as described before [19].

4.4. Inhibition of sorbitol formation in rat lenses

Male Wistar rats, 8e9 weeks old, weighting 200e250 g, were used. The animals came from the Breeding Facility of the Institute of Experimental Pharmacology and Toxicology, Dobra Voda (Slovak Republic). The study was approved by the Ethics Committee of the Institute and performed in accordance with the Principles of Lab-oratory Animal Care (NIH publication 83e25, revised 1985) and the
Slovak law regulating animal experiments (Decree 289, Part 139, July 9th, 2003). The animals in light ether anesthesia were killed by exsanguinations of the carotid artery and the eye globes were excised. The lenses were quickly dissected and rinsed with saline. Water solutions of the compounds studied were added into the tubes containing freshly dissected eye lenses (1 lens per tube) in M—199 medium (Sigma M 3769) at pH 7.4, bubbled at 37 $^{\circ}$C with pneumoxid (5% CO_2, 95% O_2), to the final concentrations as re- ported, 30 min before adding glucose. The incubation was initiated by adding glucose to the final concentration of 50 mmol/L and then continued at 37 $^{\circ}$C with occasional (in about 30 min intervals) bubbling the mixture for approximately 30 s periods with pneu-moxid. The incubations were terminated after a 3 h period by cooling the mixtures in an ice bath, followed by washing the lenses three times with ice-cold phosphate buffered saline (1 mL). The short term cultivations were preferred to avoid substantial permeability changes of the eye lenses. The washed lenses were kept deep-frozen for sorbitol determination which was performed as described before [19] (ESI).

4.3. Determination of human recombinant ALR2 activity

Materials. $_L$-idose and NADPH were from Carbosynth; GAL was from Sigma Aldrich Italy; GS-HNE was from Cayman; HNE was synthesized as previously described [38].

Purification of human recombinant ALR2. The recombinant enzyme was expressed [33] and purified [39] as previously described. The purity of the enzyme preparation was assessed by SDS-PAGE [40] and gels were stained with silver nitrate [41]; the ALR2 preparation showed a unique band corresponding to a mo-lecular weight of approximately 34 KDa. The purified ALR2 (specific activity 5.3 U/mg) was stored at 80 $^{\circ}$C in 10 mM sodium phos- phate buffer pH 7.0 (SB) containing 2 mM DTT and 30% (w/v) glycerol. The enzyme was extensively dialyzed against SB before use.

Determination of human recombinant ALR2 activity. The activity of ALR2 was determined at 37 $^{\circ}$C as previously described [42] following the decrease in absorbance at 340 nm due to NADPH oxidation (ε_{340} 6.22 mM^{-1} cm^{-1}). The standard assay mixture contained 0.25 M sodium phosphate buffer pH 6.8, 0.18 mM
NADPH, 2.4 M ammonium sulphate, 0.5 mM EDTA and 4.7 mM GAL. One unit of enzyme activity is the amount of ALR2 that catalyzes the conversion of 1 mmol of substrate/min in the above assay con- ditions. Identical assay conditions were adopted also when $_L$-idose, HNE or GS-HNE were used as substrates instead of GAL. The in- hibitors were dissolved (2.2 mM) in sodium carbonate 0.2 M and added to the assay mixture after proper dilution in the same car- bonate solution, in order to have a final carbonate concentration in the assay not higher than 3 mM. ALR2 activity was tested to be unaffected by carbonate ion up to 6 mM in the assay.

Other methods. Protein concentration was determined according to Bradford [43]. Analysis of kinetic data and statistical analysis were performed with "GraphPad 6.0". Kinetic parameters K_M and V_{max} were obtained by nonlinear regression analysis of the data. Measurements were performed at least in triplicate and reported as the mean ± the standard deviation.

References

[1] H.G. Hers, Le mécanisme de la transformation de glucose en fructose par les vésicules séminales, Biochimica Biophysica Acta. 22 (1) (1956) 202e203.
[2] P. Alexiou, et al., Aldose reductase enzyme and its implication to major health problems of the 21(st) century, Curr. Med. Chem. 16 (6) (2009) 734e752.
[3] A. Del Corso, M. Cappiello, U. Mura, From a dull enzyme to something else: facts and perspectives regarding aldose reductase, Curr. Med. Chem. 15 (15) (2008) 1452e1461.
[4] M. Brownlee, Biochemistry and molecular cell biology of diabetic complica - tions, Nature 414 (6865) (2001) 813e820.
[5] F. Giacco, M. Brownlee, Oxidative stress and diabetic complications, Circ. Res. 107 (9) (2010) 1058e1070.
[6] S. Pandey, S.K. Srivastava, K.V. Ramana, A potential therapeutic role for aldose reductase inhibitors in the treatment of endotoxin-related inflammatory diseases, Expert Opin. Investig. Drugs. 21 (3) (2012) 329e339.
[7] R. Tammali, S.K. Srivastava, K.V. Ramana, Targeting aldose reductase for the treatment of cancer, Curr. Cancer Drug Targets. 11 (5) (2011) 560e571.
[8] M. Kawamura, et al., Aldose reductase: an aldehyde scavenging enzyme in the intraneuronal metabolism of norepinephrine in human sympathetic ganglia, Auton. Neurosci. 96 (2) (2002) 131e139.
[9] M. Chatzopoulou, et al., Development of aldose reductase inhibitors for the treatment of inflammatory disorders, Expert Opin. Drug Discov. 8 (11) (2013) 1365e1380.
[10] G. Gopinath, et al., Design and synthesis of chiral 2H-chromene-N-imidazolo- amino acid conjugates as aldose reductase inhibitors, Eur. J. Med. Chem. 124 (2016) 750e762.
[11] Z. Han, et al., A series of pyrido[2,3-b]pyrazin-3(4H)-one derivatives as aldose reductase inhibitors with antioxidant activity, Eur. J. Med. Chem. 121 (2016) 308e317.
[12] Z. Iqbal, et al., Synthesis, characterization, hypoglycemic and aldose reductase inhibition activity of arylsulfonylspiro[fluorene-9,5'-imidazolidine]-2',4'-dio- nes, Eur. J. Med. Chem. 98 (2015) 127e138.
[13] M. Chatzopoulou, et al., Novel aldose reductase inhibitors: a patent survey (2006epresent), Expert Opin. Ther. Pat. 22 (11) (2012) 1303e1323.
[14] R. Maccari, R. Ottana, Targeting aldose reductase for the treatment of diabetes complications and inflammatory diseases: new insights and future directions, J. Med. Chem. 58 (5) (2015) 2047e2067.
[15] A. Del-Corso, et al., A new approach to control the enigmatic activity of aldose reductase, PLoS One 8 (9) (2013) e74076.
[16] N. Papastavrou, et al., 1-Hydroxypyrazole as a bioisostere of the acetic acid moiety in a series of aldose reductase inhibitors, Bioorg Med. Chem. 21 (17) (2013) 4951e4957.

[17]   M. Chatzopoulou, et al., Structure-activity relations on [1-(3,5-difluoro-4- hydroxyphenyl)-1H-pyrrol-3-yl]phenylmethanone. the effect of methoxy substitution on aldose reductase inhibitory activity and selectivity, Bioorg Med. Chem. 19 (4) (2011) 1426e1433.

[18]   K. Pegklidou, et al., Design and synthesis of novel series of pyrrole based chemotypes and their evaluation as selective aldose reductase inhibitors. a case of bioisosterism between a carboxylic acid moiety and that of a tetrazole, Bioorg Med. Chem. 18 (6) (2010) 2107e2114.

[19]   M. Chatzopoulou, et al., Decreasing acidity in a series of aldose reductase inhibitors: 2-fluoro-4-(1H-pyrrol-1-yl)phenol as a scaffold for improved membrane permeation, Bioorg Med. Chem. 22 (7) (2014) 2194e2207.

[20] E. Kotsampasakou, V.J. Demopoulos, Synthesis of derivatives of the keto- pyrrolyl-difluorophenol scaffold: some structural aspects for aldose reduc-tase inhibitory activity and selectivity, Bioorg Med. Chem. 21 (4) (2013) 869e873.

[21] I. Nicolaou, V.J. Demopoulos, Substituted pyrrol-1-ylacetic acids that combine aldose reductase enzyme inhibitory activity and ability to prevent the nonenzymatic irreversible modification of proteins from monosaccharides,

J. Med. Chem. 46 (3) (2003) 417e426.

[22] I. Nicolaou, V.J. Demopoulos, A study of the Friedel-Crafts acylation of 1- benzenesulfonyl-1H-pyrrole   in   the   preparation   of   3-aroylpyrroles, J. Heterocycl. Chem. 35 (6) (1998) 1345e1348.

[23] J. Pawlas, et al., Synthesis of 1-hydroxy-substituted pyrazolo[3,4-c]- and pyrazolo[4,3-c]quinolines and -isoquinolines from 4- and 5-aryl-substituted 1-benzyloxypyrazoles, J. Org. Chem. 65 (26) (2000) 9001e9006.

[24] M. Andres, et al., 2-(1H-Pyrazol-1-yl)acetic acids as chemoattractant receptor- homologous molecule expressed on Th2 lymphocytes (CRTh2) antagonists, Eur. J. Med. Chem. 71 (2014) 168e184.

[25] V.J. Demopoulos, E. Rekka, Isomeric benzoylpyrroleacetic acids: some struc- tural aspects for aldose reductase inhibitory and anti-inflammatory activities, J. Pharm. Sci. 84 (1) (1995) 79e82.

[26] B.R. Beno, et al., A survey of the role of noncovalent sulfur interactions in drug design, J. Med. Chem. 58 (11) (2015) 4383e4438.

[27] X. Zheng, et al., The molecular basis for inhibition of sulindac and its me- tabolites towards human aldose reductase, FEBS Lett. 586 (1) (2012) 55e59.

[28] K.J. Rees-Milton, et al., Aldehyde reductase: the role of C-terminal residues in defining substrate and cofactor specificities, Arch. Biochem. Biophys. 355 (2) (1998) 137e144.

[29] I. Nicolaou, C. Zika, V.J. Demopoulos, [1-(3,5-difluoro-4-hydroxyphenyl)-1H- pyrrol-3-yl]phenylmethanone as a bioisostere of a carboxylic acid aldose reductase inhibitor, J. Med. Chem. 47 (10) (2004) 2706e2709.

[30] O. Trott, A.J. Olson, AutoDock Vina: improving the speed and accuracy of docking with a new scoring function, efficient optimization, and multi- threading, J. Comput. Chem. 31 (2) (2010) 455e461.

[31] G.M. Morris, et al., AutoDock4 and AutoDockTools4: automated docking with selective receptor flexibility, J. Comput. Chem. 30 (16) (2009) 2785e2791.

[32] I. Musmuca, et al., Combining 3-d quantitative structure activity relationship with ligand based and structure based alignment procedures for in silico screening of new hepatitis C virus NS5B polymerase inhibitors, J. Chem. Inf.

Model. 50 (4) (2010) 662e676.

[33] F. Balestri, et al., L-Idose: an attractive substrate alternative to D-glucose for measuring aldose reductase activity, Biochem. Biophys. Res. Commun. 456 (4) (2015) 891e895.

[34] M. Cappiello, et al., Basic models for differential inhibition of enzymes, Bio- chem. Biophys. Res. Commun. 445 (3) (2014) 556e560.

[35] A.L. Hopkins, et al., The role of ligand efficiency metrics in drug discovery, Nat. Rev. Drug Discov. 13 (2) (2014) 105e121.

[36] K. Palm, et al., Polar molecular surface properties predict the intestinal ab- sorption of drugs in humans, Pharm. Res. 14 (5) (1997) 568e571.

[37] E. Perola, An analysis of the binding efficiencies of drugs and their leads in successful drug discovery programs, J. Med. Chem. 53 (7) (2010) 2986e2997.

[38] R. Moschini, et al., NADP( )-dependent dehydrogenase activity of carbonyl reductase on glutathionylhydroxynonanal as a new pathway for hydrox- ynonenal detoxification, Free Radic. Biol. Med. 83 (2015) 66e76.

[39] F. Balestri, et al., Modulation of aldose reductase activity by aldose hemi- acetals, Biochim. Biophys. Acta. 1850 (11) (2015) 2329e2339.

[40] U.K. Laemmli, Cleavage of structural proteins during the assembly of the head of bacteriophage T4, Nature 227 (5259) (1970) 680e685.

[41] W. Wray, et al., Silver staining of proteins in polyacrylamide gels, Anal. Bio- chem. 118 (1) (1981) 197e203.

[42] F. Balestri, et al., Zolfino landrace (Phaseolus vulgaris L.) from Pratomagno: general and specific features of a functional food, Food Nutr. Res. 60 (2016) 31792.

[43] M.M. Bradford, A rapid and sensitive method for the quantitation of micro- gram quantities of protein utilizing the principle of protein-dye binding, Anal. Biochem. 72 (1976) 248e254

i